Adaptive numerical simulation of turbulent premixed combustion

J. B. Bell, M. S. Day, A. S. Almgren, M. J. Lijewski and C. A. Rendleman

Lawrence Berkeley National Laboratory
Berkeley, CA, 94720

Abstract. We describe an adaptive algorithm for low Mach number reacting flows with complex chemistry in three dimensions. Our approach uses a form of the low Mach number equations that discretely conserves both mass and energy. The discretization methodology is based on a robust projection formulation that accommodates large density contrasts. The algorithm uses an operator-split treatment of stiff reaction terms and includes effects of differential diffusion. The basic computational approach is embedded in an adaptive projection framework based on structured hierarchical grids with subcycling in time that preserves the discrete conservation properties of the underlying single-grid algorithm. We apply the methodology to the simulation of a premixed turbulent hydrogen flame.

Keywords: Projection methods, low Mach number flows, premixed combustion, turbulence

1. Introduction

Detailed modeling of turbulent reacting flows in three dimensions with realistic chemical mechanisms places severe demands on computational resources. One approach to reducing this computational cost is the of use of local adaptive mesh refinement to reduce the total number of computational zones that must be advanced for a specific problem. There is an extensive literature on adaptive methods for modeling reacting flows. The reader is referred to Bennett and Smooke [1], Najm *et al.* [2] and Day and Bell [3] for a survey of this literature. The methodology presented here generalizes that presented in Day and Bell [3] to three dimensions. This approach is based on a variable density projection formulation and uses second-order Godunov-type upwind methodology for advective transport. Chemical kinetics are included in the numerical advance using a second-order operator-split approach.

2. Mathematical Model

Our model is based on a conservative form of the low Mach number combustion model introduced by Rehm and Baum [4], subsequently derived from low Mach number asymptotic analysis by Majda and Sethian [5]. We consider a gaseous mixture, ignoring Soret and Dufour effects, body forces and radiative heat transfer, and assume a mixture model for species diffusion [6,7]. For an unconfined domain, we have

$$\frac{\partial \rho U}{\partial t} + \nabla \cdot \rho U U = -\nabla \pi + \nabla \cdot \tau, \tag{1}$$

$$\frac{\partial \rho Y_m}{\partial t} + \nabla \cdot U \rho Y_m = \nabla \cdot \rho \mathcal{D}_m \nabla Y_m + \dot{\omega}_m, \tag{2}$$

$$\frac{\partial \rho h}{\partial t} + \nabla \cdot U \rho h = \nabla \cdot \lambda \nabla T + \sum_m \nabla \cdot \rho h_m(T) \mathcal{D}_m \nabla Y_m \tag{3}$$

where ρ is the density, U is the velocity, π is the pressure variation from a uniform ambient pressure, Y_m is the mass fraction of species m, h is the mass-weighted enthalpy of the gas mixture, T is the temperature, and $\dot{\omega}_m$ is the net production rate for species m due to chemical reactions. Also, λ is the thermal conductivity, τ is the stress tensor, $c_{p,mix}$ is the specific heat of the mixture and $h_m(T)$ and $\mathcal{D}_m$ are the enthalpy and species mixture-averaged diffusion coefficients of species m, respectively. These evolution equations are supplemented by an equation of state for a perfect gas mixture:

$$p_0 = \rho R_{mix} T = \rho \mathcal{R} T \sum_m \frac{Y_m}{W_m} \tag{4}$$

where W_m is the molecular weight of species m.

In the low Mach number limit, the thermodynamic pressure given by equation (4) remains approximately constant as the flow evolves. Differentiating the equation of state in the frame of the fluid, and using the conservation equations to replace advective derivatives, we obtain a constraint on the evolving velocity field:

$$\begin{aligned} \nabla \cdot U = & \frac{1}{\rho c_p T} \left(\nabla \cdot \lambda \nabla T + \sum_m \rho \mathcal{D}_m \nabla Y_m \cdot \nabla h_m \right) + \\ & + \frac{1}{\rho} \sum_m \frac{W}{W_m} \nabla \cdot \rho \mathcal{D}_m \nabla Y_m \; - \frac{1}{\rho} \sum_m \left(\frac{h_m(T)}{c_{p,mix} T} - \frac{W}{W_m} \right) \dot{\omega}_m \equiv S \end{aligned} \tag{5}$$

where $W = (\sum_m Y_m / W_m)^{-1}$ and $c_{p,mix} = \sum_m Y_m dh_m/dT$.

3. Numerical methodology

Our computational approach uses a hierarchical adaptive mesh refinement (AMR) algorithm based on an approximate projection formulation for integrating the momentum equations developed by Almgren *et al.* [8], and subsequently extended to low Mach number reacting flows by Pember *et al.* [9]. The projection algorithm is coupled to conservation equations for chemical species and enthalpy. The single-grid algorithm is implemented in a structured uniform grid setting, and incorporated into an AMR framework that employs a recursive time-stepping procedure over refinement levels. We sketch the numerical implementation below; the reader is referred to Day and Bell [3] for details.

The single-grid scheme is a fractional step algorithm that first advances momentum, species and enthalpy equations with a lagged perturbational pressure. We discretize equations (1–3) using a second-order Godunov scheme for the convective terms and a time-centered Crank-Nicolson discretization for diffusion. The Godunov discretization incorporates in intermediate projection so that the velocity field used to compute the advective derivatives satisfies the constraint (5). Because the transport coefficients depend on both temperature and composition, we adopt a sequential, predictor-corrector scheme to guarantee second-order treatment of nonlinear diffusion effects. The chemistry is advanced using time-implicit backward differentiation methods in VODE [10]. The advection/diffusion and chemistry components of the algorithm are time-split symmetrically to ensure that the composite algorithm remains second-order.

The velocity field resulting from the advection/diffusion/chemistry step is then projected using a density-weighted approximate projection to enforce the velocity divergence constraint (5). Numerically, the projection step requires the solution of a variable-coefficient linear elliptic equation. In addition to enforcing the divergence constraint, the projection also determines an update to the perturbational pressure. The explicit procedure for the treatment of advection terms necessitates a CFL-type time-step restriction. Since the advective time scale is typically larger than the fastest time scales associated with the chemical kinetics, this does not appear to be a serious disadvantage for time-dependent simulations.

We note that because of the fractional step nature of the overall approach, it is impossible to satisfy the equation of state while conserving species and enthalpy discretely. To control the deviation from the equation of state we incorporate a correction to the constraint (5) of the form

$$\frac{f}{\gamma p_{amb}} \left(\frac{\delta p}{\Delta t} + U \cdot \nabla p \right).$$

into the intermediate projection used to compute the velocity field required to evaluate convective derivatives. Here $\delta p = p_0 - p_{amb}$, where p_0 is defined discretely from equation (4), p_{amb} is the specified ambient pressure, Δt is the numerical time step, γ is the local ratio of specific heats. and the sum $\frac{\delta p}{\Delta t} + U \cdot \nabla p$ is a first-order approximation to the material derivative of $p_0 - p_{amb}$ along streamlines. This forcing term prevents the solution from deviating an appreciable amount from the equation of state while maintaining the second-order accuracy of the overall scheme. The details of an earlier version of this correction, and its effects, are discussed in [3].

The extension of the above algorithm to adaptive mesh refinement is based on a hierarchical refinement strategy. Our methodology uses a system of overlaid grids with successively finer spacing in time and space. Fine grids are formed by uniformly dividing coarse cells in each direction. Increasingly finer levels, each consisting of a union of rectangular grid patches, overlay underresolved portions of the coarser grid levels until the solution is adequately resolved. An error estimation procedure identifies where refinement is needed and grid generation procedures dynamically create or remove rectangular fine grid patches as the solution is evolved and requirements change.

The complete adaptive algorithm has a number of desirable properties. The overall method is second-order accurate in space and time, and discretely conserves species mass and enthalpy. Furthermore, the algorithm satisfies a free-stream preservation property so that nonreacting isothermal flow remains numerically isothermal during species transport.

The methodology has been implemented for distributed memory parallel processors using the BoxLib class libraries described by Rendleman *et al.* [11]. In this approach, grid patches are distributed to processors using a heuristic knapsack algorithm to balance the computational work (see Crutchfield [12]). For nonreacting fluid flows, work estimates based on the number of cells in a grid provide an effective load balancing strategy. However, for reacting flows there can be considerable variability in the time required to integrate the kinetics equations depending on temperature and composition. To account for this variability we monitor the number of rate evaluations required to integrate the kinetics equations and use the data to estimate the work required to advance the chemistry for each grid patch. These estimates are used for a separate, finer-grained load balancing step for the chemistry.

4. Results

To test the methodology, we have applied it to the simulation of a turbulent, premixed hydrogen flame. The nine-species hydrogen chemistry model is formed by extracting the relevant twenty-seven reactions from the GRI-1.2 [13]. The basic flow configuration, as depicted in Figure 1, has inflow at the bottom, outflow at the top and is periodic in the remaining directions. The flow is initialized using a premixed hydrogen flame with an inflow velocity for which the resulting laminar flame is stationary. At the inflow face we impose a time-dependent perturbation to the velocity boundary condition representing three-dimensional, decaying isotropic turbulence. The energy spectrum of the turbulence is specified by

$$E(k) = C * (k^4/{k_o}^5) exp(-2 * (k/k_o)^2)$$

where k_o is the peak frequency ($12 cm^{-1}$ here) and C is a constant used to specify the turbulent intensity which we take to be five times the laminar flame speed.

The computation was performed on a $32{\times}32{\times}128$ base grid. Two additional levels of dynamic refinement, covering less than 20% of the domain, resulted in a effective grid resolution of $128{\times}128{\times}512$ near the flame front and the inflow face. As the flow evolves the inflow turbulence reaches and begins to interact with the flame. A volume-rendered image showing the location and shape of the flame front at the end of the computation is presented in Figure 2.

5. Conclusions

We have demonstrated that adaptive mesh refinement can be applied effectively to high-resolution simulations of turbulent, premixed combustion. The overall utility of the approach depends on the relative size of the length scales present in the flame and the length scales associated with the turbulent flow. Another critical issue is the development of robust error estimation criteria that can effectively control the adaptation to ensure a required level of accuracy. These issues will be addressed in future work.

Acknowledgments

This work was supported by the Applied Mathematics Program of the DOE Office of Mathematics, Information, and Computational Sciences under the U.S. Department of Energy under contract No. DE-AC03-76SF00098.

[1] Bennett, B.A.V. and Smooke, M. D., *J. Comput. Phys.*, 151(2):684–727 (1999).

[2] Najm, H.N., Schefer, R.W., Milne, R.B., Mueller, C.J., Devine, K.D., and Kempka, S.N., "Numerical and experimental investigation of vortical flow–flame interaction," Sandia National Laboratory Report No. SAND98-8232.

[3] Day, M. S. and Bell, J. B., *Combust. Theory Model*, 4:535–556 (2000).

[4] Rehm, R.G. and Baum, H.R., *N.B.S.J.Res.*, 83:297–308 (1978).

[5] Majda, A. and Sethian, J. A., *Combust. Sci. Tech.*, 42:185–205 (1985).

[6] Kee, R. J., Dixon-Lewis, G., Warnatz, J., Coltrin, M. E., and Miller, J. A., "A FORTRAN computer code package for the evaluation of gas-phase multicomponent transport properties," Sandia National Laboratories Report No. SAND86-8246.

[7] Warnatz, J., (Peters, N. and Warnatz, J., editors), *Numerical methods in flame propagation*, Friedr. Viewweg and Sohn, Wiesbaden, 1982.

[8] Almgren, A. S., Bell, J. B., Colella, P., Howell, L. H., and Welcome, M., *J. Comput. Phys.*, 142:1–46 (1998).

[9] Pember, R. B., Howell, L. H., Bell, J. B., Colella, P., Crutchfield, W. Y., Fiveland, W. A., and Jessee, J. P., *Comb. Sci. Tech.*, 140:123–168 (1998).

[10] Brown, P. N., Byrne, G. D., and Hindmarsh, A. C., *SIAM J. Sci. Stat. Comput.*, 10:1038–1051 (1989).

[11] Rendleman, C. A., Beckner, V. E., Lijewski, M., Crutchfield, W. Y., and Bell, J. B., *Computing and Visualization in Science*, (2000), Appears also as Lawrence Berkeley National Lab Report LBNL-43154.

[12] Crutchfield, W. Y., "Load balancing of an irregular algorithm," LLNL Report No. UCRL-JC-107679.

[13] Frenklach, M., Wang, H., Goldenberg, M., Smith, G. P., Golden, D. M., Bowman, C. T., Hanson, R. K., Gardiner, W. C., and Lissianski, V., "GRI-Mech—An optimized detailed chemical reaction mechanism for methane combustion," Gas Research Institute Report No. GRI-95/0058, See also `http://www.me.berkeley.edu/gri_mech/`.

Figure Captions

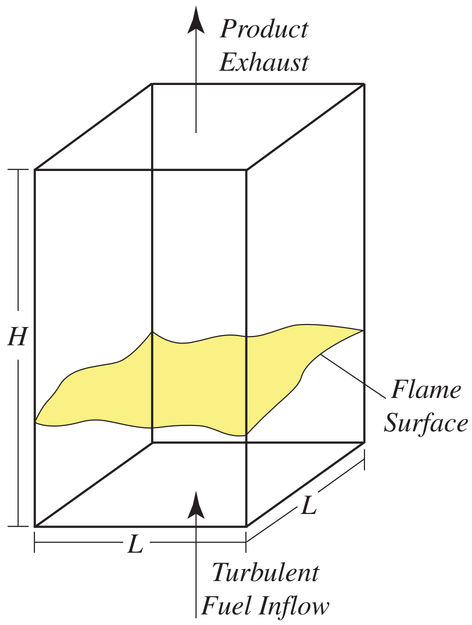

Figure 1. Schematic of the flow configuration used for simulating the interaction of isotropic turbulence with a premixed hydrogen flame. Here, $L = 5mm$, and $H = 10mm$.

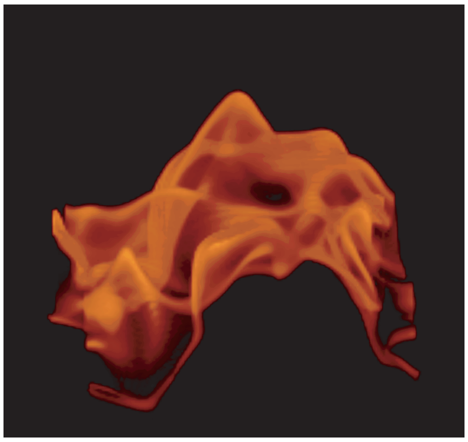

Figure 2. Surface of the premixed hydrogen flame (marked by the flame radical, HO2) perturbed by a turbulent inflow stream from the bottom of the domain.